iScience

CellPress
OPEN ACCESS

Article

circIFNGR2 regulating ankylosing spondylitis-associated inflammation through macrophage polarization

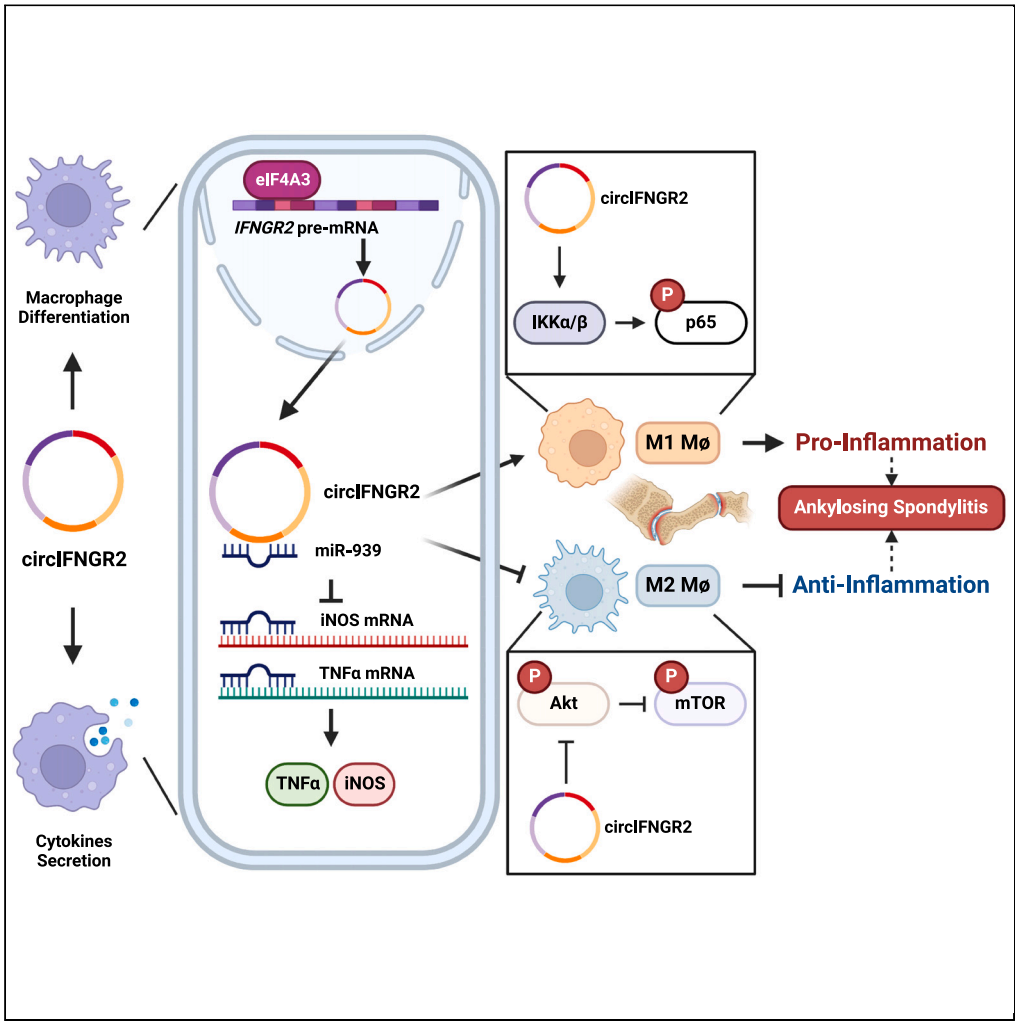

Minkai Song, Xiangyu Wang, Jiawen Gao, ..., Zhanjun Shi, Jun Xiao, Chao Zhang

xiaojun@smu.edu.cn (J.X.)
super1998@smu.edu.cn (C.Z.)

Highlights

CircIFNGR2 is associated with disease status of ankylosing spondylitis

CircIFNGR2 promotes M1 macrophage but restrains M2 macrophage polarization

EIF4A3-induced circIFNGR2 regulates macrophage-associated inflammation via miR-939

CircIFNGR2/miR-939 collaboratively regulated inflammatory arthritis

Song et al., iScience 26, 107325
August 18, 2023
https://doi.org/10.1016/j.isci.2023.107325

iScience

CellPress
OPEN ACCESS

Article

circIFNGR2 regulating ankylosing spondylitis-associated inflammation through macrophage polarization

Minkai Song,[1,6] Xiangyu Wang,[2,6] Jiawen Gao,[3,6] Weizhou Jiang,[1] Enguang Bi,[4] Taixue An,[5] Ting Wang,[4] Zishuo Chen,[4] Weilu Liu,[1] Zhanjun Shi,[1] Jun Xiao,[1,*] and Chao Zhang[4,7,*]

SUMMARY

Macrophages activation is crucial in pathogenesis of rheumatic diseases like ankylosing spondylitis (AS). Circular RNAs (circRNAs)-induced macrophage-associated inflammation participates in many autoimmune diseases but remains elusive in AS. Here, we verified increased expression of circIFNGR2 in peripheral blood mononuclear cells from patients with AS and its expression levels were correlated with the AS severity. *In vitro* assays revealed that circIFNGR2 enhances macrophage proliferation, and regulates M1/M2 macrophage polarization and NF-κB/Akt pathways. We identified that circIFNGR2 promoted the expression of iNOS/TNFα and M1 polarization, and restrained M2 polarization by sponging miR-939. Additionally, the RNA-binding protein, eIF4A3, was found to enhance the production of circIFNGR2. Interestingly, miR-939 attenuated joint damage in collagen-induced arthritis mice, whereas circIFNGR2 reversed this effect. Our findings highlight the pro-inflammatory roles of eIF4A3-induced circIFNGR2 in AS by modulating macrophage-associated inflammation through miR-939.

INTRODUCTION

Ankylosing spondylitis (AS) is a common autoimmune disease characterized by inflammatory back pain, irreversible damage to small joints, and a high prevalence of HLA-B27 in young adults.[1] Sustained abnormal inflammation has been identified as the culprit of arthritis and varied extra-articular manifestations in AS.[2] Extensive research studies suggested that the activation of antigen-processing cells (APCs) and the subsequent activation of T cells are main causes of AS-associated inflammation.[3] Among pro-inflammatory APCs, macrophages play essential roles in variety of rheumatic diseases such as rheumatoid arthritis (RA), psoriatic arthritis, and juvenile idiopathic arthritis.[4] Typically, macrophages in autoimmune diseases have been categorized as two subsets including classical activated macrophages (M1) with pro-inflammatory effects on tissue damage, and alternative macrophages (M2) with anti-inflammatory effects on injury repair.[5] Our previous study found a greater proportion of $CD14^+$ cells in peripheral blood mononuclear cells (PBMCs) from patients with AS than in healthy controls, indicating that monocytes/macrophages might involve in pathogenesis of AS.[6] Unfortunately, the precise functions and regulation of M1/M2 macrophages in AS have not yet been fully elucidated.

Circular RNAs (circRNAs) are non-coding RNAs with a unique structural characteristic as a covalently closed loop without 3′ polyadenylated tail or 5′ cap.[7] Mounting data have shown that circRNAs participated in the progression of osteoarthritis, RA, systemic lupus erythematosus, and many other rheumatic diseases.[8–11] Notably, circRNAs are also crucial in activation of macrophages in many inflammatory diseases.[12–14] Previously, we identified the differential expression of circRNAs in PBMCs from patients with AS and clarified the role of hsa_circ_0000652 in trigging inflammatory reactions between macrophage and $CD4^+$ T cells.[6] Nevertheless, the comprehensive understandings of circRNA-regulated macrophage activation in AS require further exploration.

Back-splicing is the fundamental procedure in biogenesis of matured circRNAs. During the transcription of genes, some RNA-binding proteins (RBPs) can bind to upstream or downstream introns of pre-mRNA and facilitate the back-splicing.[15] eIF4A3 has been reported to be involved in regulation of circRNA biogenesis.[16] Meanwhile, it has been reported that eIF4A3 itself participated in progression of various disease

[1]Division of Orthopaedic Surgery, Department of Orthopaedics, NanFang Hospital, Southern Medical University, Guangzhou, China

[2]Department of Endocrinology & Metabolism, NanFang Hospital, Southern Medical University, Guangzhou, China

[3]Division of Spinal Surgery, Department of Orthopaedics, NanFang Hospital, Southern Medical University, Guangzhou, China

[4]Department of Biochemistry and Molecular Biology, School of Basic Medical Science, Guangdong Provincial Key Laboratory of Single Cell Technology and Application, Southern Medical University, Guangzhou, China

[5]Department of Laboratory Medicine, NanFang Hospital, Southern Medical University, Guangzhou, China

[6]These authors contributed equally

[7]Lead contact

*Correspondence: xiaojun@smu.edu.cn (J.X.), super1998@smu.edu.cn (C.Z.)

https://doi.org/10.1016/j.isci.2023.107325

including glioblastomas, colorectal cancer, and type 1 diabetes mellitus.[14,17,18] However, the roles of eIF4A3 in AS and its regulation on AS-specific circRNAs are beyond discovery.

Here, we revealed the expression profiles and pro-inflammatory effects of circIFNGR2 in regulating AS-associated inflammation through macrophage polarization. Mechanically, eIF4A3-induced circIFNGR2 was proved to regulate the expression of iNOS/TNFα, M1/M2 polarization, and NF-κB/Akt pathways of macrophages by sponging and suppressing miR-939, thereby enhancing the inflammation and development of AS. This research uncovers the pro-inflammatory roles and regulatory networks of circIFNGR2 in AS, and provides a potential approach for treatment targeting macrophage-associated inflammation of AS.

RESULTS

circIFNGR2 is differentially expressed in AS and correlated with disease activity

We previously identified differentially expressed circRNAs via high-throughput circRNA sequencing using PBMCs from patients with AS and healthy controls.[6] Among the differentially expressed circRNAs, circIFNGR2 showed the characteristics with 124.53-fold changes and p value = 0.003. In the present study, qRT-PCR analysis revealed that circIFNGR2 had an elevated expression level in patients with AS with $ASDAS_{CRP}$ score $\geq$2.1 compared to health controls by (Figure 1A). We further found that the expression level of circIFNGR2 in patients with AS with high disease activity (AS-HDA, 2.1 $\leq$ $ASDAS_{CRP}$ score $<$ 3.5) was higher than healthy controls, while less than the patients with AS with very high disease activity (AS-VHDA, $ASDAS_{CRP}$ score $\geq$3.5) (Figure 1B). To clarify the potential clinical significance of circIFNGR2, we used correlation analysis to determine the correlation between expression level of circIFNGR2 and multiple disease activity indexes. As the results shown in Figures 1C–1E, the expression level of circIFNGR2 of patients with AS has positive correlations with $ASDAS_{CRP}$ score, BASDAI score, and serum C-reactive protein levels, respectively. These findings indicated that circIFNGR2 was upregulated in PBMCs of patients with AS and correlated with clinical disease activity, suggesting that circIFNGR2 may be involved in the pathogenesis of AS.

Validation of circIFNGR2

According to bioinformatic analysis, circIFNGR2 was generated by back-splicing from exon 2 to exon 6 of linear pre-mRNA of IFNGR2 (Figure 1F). Sanger sequencing was used for the validation of sequences near back-splicing joint of circIFNGR2 (Figure 1G). Since circRNAs can be amplified from cDNA but not from gDNA, we designed convergent and divergent primers of circIFNGR2 to perform PCR reaction in cDNA and gDNA. Results from agarose gel electrophoresis showed that convergent primers of circIFNGR2 were able to amplify with both cDNA and gDNA, while divergent primers amplified only with cDNA (Figure S1). To further validate the circular structural characteristic of circIFNGR2, we detected PCR products from RNA treated with or without RNase R and found that circIFNGR2 had greater stability than linear IFNGR2 (Figure 1I). Moreover, qRT-PCR analysis of nuclear RNA and cytoplasmic RNA indicated that circIFNGR2 was primarily located in cytoplasm of macrophages (Figure 1J).

circIFNGR2 regulates M1/M2 polarization and NF-κB/Akt activation

To study the potential roles of circIFNGR2 in immune cells, we firstly identified that circIFNGR2 was mainly located in peripheral blood $CD14^+$ cells rather than $CD14^-$ cells of PBMCs (Figure 2A). As $CD14^+$ cells can be differentiated to macrophages, we used qRT-PCR analysis in different polarization stage of macrophages and found that the expression level of circIFNGR2 elevated in M1 macrophages but decreased in M2 macrophages (Figure 2B). To further determine the biofunctions of circIFNGR2, we used lentivirus to construct stably expressed THP-1 cells with overexpression or knockdown of circIFNGR2 and qRT-PCR was used to verify the effectiveness (Figure 2C). Next, we conducted EdU proliferation assays and found that overexpression of circIFNGR2 augmented the proliferation rate of THP-1 cells while knockdown of circIFNGR2 diminished the proliferation (Figures 2D and 2E). After the treatment of M1 polarization, THP-1-derived macrophages with overexpression of circIFNGR2 showed an increased proportion of the $iNOS^+TNF\alpha^+$ cells than control, while knockdown of circIFNGR2 resulted in restrain of $iNOS^+TNF\alpha^+$ cells (Figures 2F and 2G). qRT-PCR and Western blot analysis also demonstrated that overexpression of circIFNGR2 significantly enhanced the expression levels of iNOS, CD86, IL1β, IL6, and TNFα in THP-1-derived M1 macrophages, while knockdown of circIFNGR2 resulted conversely (Figures S2, 2H and 2I). As NF-κB pathway is critical pro-inflammatory stimuli in M1 macrophage, we performed Western blot analysis to

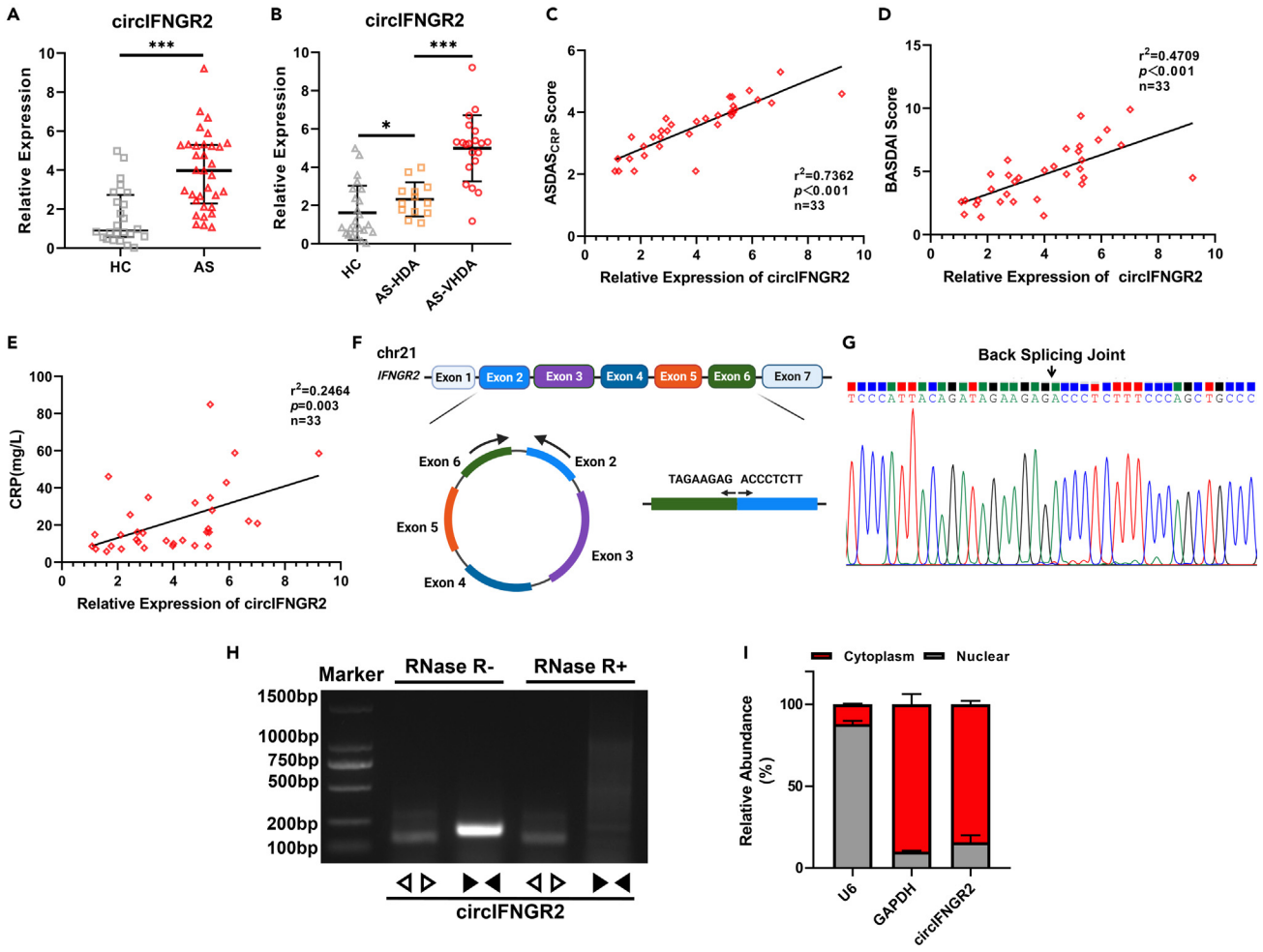

Figure 1. circIFNGR2 was upregulated in PBMCs from patients with AS and correlated with disease activity

(A and B) qRT-PCR analysis of the expression of circIFNGR2 in PBMCs from 24 healthy controls and 33 patients with AS including 13 patients with high disease activity (HDA, 2.1 ≤ ASDAS$_{CRP}$ score < 3.5) and 20 patients with very high disease activity (VHDA, ASDAS$_{CRP}$ score ≥ 3.5).

(C–E) Correlation analysis of ASDAS$_{CRP}$ score, BASDAI score, and serum CRP levels and the expression levels of circIFNGR2 in PBMCs from patients with AS.

(F) Schematic illustration of structural characteristics and back-splicing junction of circIFNGR2.

(G) The back-splicing junction sequences of circIFNGR2 were validated by Sanger sequencing.

(H) RT-PCR amplification of circIFNGR2 and linear IFNGR2 in THP-1 cells treated with or without RNase R.

(I) qRT-PCR analysis of the expression level of circIFNGR2, U6, and GAPDH in nuclear-cytoplasm separation assay. Data in A and B are presented as median ± quartile, data in F and K are presented as mean ± SD. ***: $p < 0.001$.

detect the expression change led by circIFNGR2. As the results presented in Figures 2J and 2K, phosphorylation and nuclear import of p65, and the expression level of Ikkα/β were remarkably enhanced in THP-1-derived M1 macrophages with overexpression of circIFNGR2 but reversed by knockdown of circIFNGR2 (Figures 2J and 2K). Moreover, results from ELISA assays also showed that the secretion levels of TNFα, IL6, IL1β, and IL23 were significantly increased in M1 macrophages with overexpression of circIFNGR2, while decreased in M1 macrophages with knockdown of circIFNGR2 (Figures 2L–2O). Accordingly, these data revealed that circIFNGR2 promoted proliferation, M1 polarization, and the secretion of pro-inflammatory cytokines of macrophages.

Since polarization of macrophages is not strictly irreversible *in vivo*, we next investigated the effects of circIFNGR2 in THP-1-derived M2 macrophages. Interestingly, flow cytometry analysis displayed that overexpression of circIFNGR2 diminished the proportion of CD163$^+$CD206$^+$ cells under the conditions of M2 macrophage polarization, while knockdown of circIFNGR2 showed opposite effects (Figures 2P and 2Q). Akt pathway has previously reported to have critical role in the process of M2 polarization. As expected,

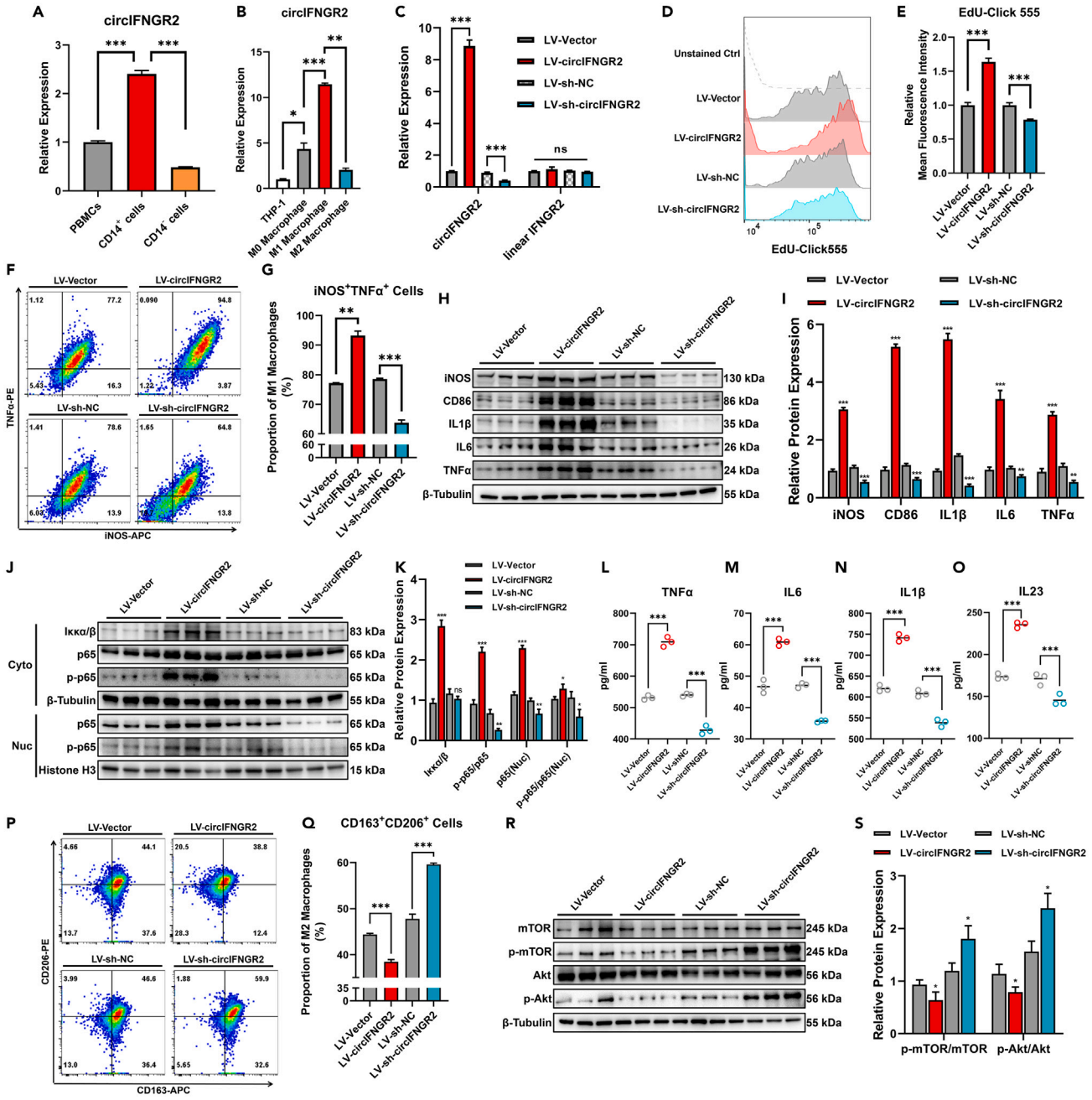

Figure 2. circIFNGR2 enhanced M1 macrophage polarization and restrained M2 macrophage polarization

(A) qRT-PCR analysis of the expression level of circIFNGR2 in total PBMCs, peripheral $CD14^+$ cells, and peripheral $CD14^-$ cells.

(B) qRT-PCR analysis of the expression level of circIFNGR2 in THP-1 cells, M0 macrophages, M1 macrophages and M2 macrophages.

(C) qRT-PCR analysis of the expression levels of circIFNGR2 and linear IFNGR2 in circIFNGR2 stably transfected THP-1 cells.

(D and E) Flow cytometry analysis for EdU proliferation assays in THP-1 cells with overexpression or knockdown of circIFNGR2.

(F and G) Flow cytometry analysis of iNOS+TNFα+ cells in THP-1-derived M1 macrophages with overexpression and knockdown of circIFNGR2.

(H and I) Western Blot analysis of relative protein expression of iNOS, CD86, IL1β, IL6, and TNFα in THP-1-derived M1 macrophages with overexpression and knockdown of circIFNGR2.

(J and K) Western Blot analysis of relative protein expression of cytoplasmic Ikkα/β, total p65 and phosphorylated p65, and nuclear p65 in THP-1-derived M1 macrophages with overexpression and knockdown of circIFNGR2.

(L–O) ELISA analysis of the secretion levels of TNFα, IL6, IL1β, and IL23 in THP-1-derived M1 macrophages with overexpression and knockdown of circIFNGR2.

Figure 2. *Continued*

(P and Q) Flow cytometry analysis of CD163+CD206+ cells in THP-1-derived M2 macrophages with overexpression and knockdown of circIFNGR2.

(R and S) Western Blot analysis of relative protein expression of total mTOR, phosphorylated mTOR, total Akt, and phosphorylated Akt in THP-1-derived M2 macrophages with overexpression and knockdown of circIFNGR2. Data in bar plots are presented as mean ± SD, data in scatterplots are supplemented with line of mean. *: $p < 0.05$; **: $p < 0.01$; ***: $p < 0.001$; ns: $p \geq 0.05$.

results from Western blot analysis demonstrated that overexpression of circIFNGR2 caused restraint of phosphorylation of Akt and mTOR in M2 macrophages but knockdown of circIFNGR2 enhanced the activation of Akt and mTOR (Figures 2R and 2S). In short, these findings suggested that circIFNGR2 suppressed M2 polarization and attenuated Akt/mTOR activation in macrophages.

EIF4A3 regulates the expression of circIFNGR2

It has been previously reported that some of RBPs are able to bind to the flanking intron sequences of pre-mRNA of circRNA host gene and regulate the expression of circRNA.[19] To explore whether RBPs involved in biogenesis of circIFNGR2, we firstly analyzed with circInteractome database and found three putative binding sites of eIF4A3 in flanking sequences of circIFNGR2 as sequence a, b, and c (Figure 3A). Results from RIP assays showed that eIF4A3 could bind to sequence a and c of flanking sequences of circIFNGR2 but not to sequence b and matured circIFNGR2 (Figure 3B). To further verify the binding relationships, RAP assays using probes targeted sequence a and c were conducted and the results demonstrated that sequence a from upstream and sequence c from downstream of circIFNGR2 could both bind to eIF4A3 (Figure 3C). Hence, we speculated that eIF4A3 might interfere with the biogenesis by binding to the flanking sequences. Since circIFNGR2 primarily located in monocytes/macrophages, we performed qRT-PCR analysis and found that the expression level of eIF4A3 elevated in M1 macrophages but decreased in M2 macrophages, which shared similar patterns as circIFNGR2 (Figure 3D). Next, we transfected THP-1-derived macrophages with plasmids containing coding sequences of eIF4A3 and siRNAs targeting eIF4A3, respectively. Results from qRT-PCR analysis displayed that independent to linear IFNGR2, the expression level of circIFNGR2 was significantly elevated with overexpression of eIF4A3 but diminished with knockdown of eIF4A3, indicating that eIF4A3 specifically facilitated the cyclization of circIFNGR2 (Figure 3E). Furthermore, we detected the expression levels of eIF4A3 in PBMCs samples from patients with AS and healthy controls and the results revealed that eIF4A3 was upregulated in patients with AS and correlated with the expression levels of circIFNGR2 (Figures 3F and 3G). Taken together, eIF4A3 promoted the expression of circIFNGR2 by binding to its flanking sequences.

circIFNGR2 serves as a sponge for miR-939

Given that cytoplasmic circRNAs can regulate target genes by repressing miRNAs as ceRNA,[15] we used circInteractome and TargetScan database to predict the potential targets of circIFNGR2 and chose miR-939 for further study (Figure 4A). qRT-PCR analysis showed that the expression level of miR-939 was notably diminished in PBMCs from patients with AS compared to healthy controls (Figure 4B). In contrast to circIFNGR2, we found that the expression level of miR-939 in patients with AS with high disease activity was lower than healthy controls, while higher than the patients with AS with very high disease activity (Figure 4C). Correlation analysis demonstrated that the expression level of miR-939 was negatively correlated with $ASDAS_{CRP}$ score and the expression of circIFNGR2 (Figures 4D and 4E). Nevertheless, the correlation between the expression level of miR-939 and BASDAI score, or serum C-reactive protein level statistically did not show any significance (Figure S3). To identify the role of miR-939 in macrophages, we performed qRT-PCR analysis in different stages of macrophages and found that miR-939 was downregulated in M1 macrophages while upregulated in M2 macrophages, indicating that miR-939 might play an anti-inflammatory role in macrophage polarization (Figure 4F). Since the expression patterns of miR-939 contrasted to circIFNGR2, we assumed that circIFNGR2 had the potential to act as a sponge for miR-939. Consequently, we separately conducted RAP assays with biotin-labeled probes targeted circIFNGR2 and miR-939 to verify the binding interaction. Results from the RAP assays exhibited that miR-939 was enriched by probes of circIFNGR2 and circIFNGR2 was also enriched by probes of miR-939 (Figures 4G and 4H). Additionally, dual-luciferase reporter assays also demonstrated that miR-939 significantly attenuated the luciferase activity of circIFNGR2 wild-type group compared to control and mutant group (Figures 4I and 4J). Accordingly, these experiments confirmed that circIFNGR2 could bind to miR-939. To clarify the regulatory effect of circIFNGR2 and miR-939, we used qRT-PCR to test the expression levels of circIFNGR2 and miR-939 in cells with overexpression and knockdown of circIFNGR2 or miR-939, respectively. Indeed, we found that overexpression of circIFNGR2 resulted in decrease of the expression of miR-939, while knockdown of

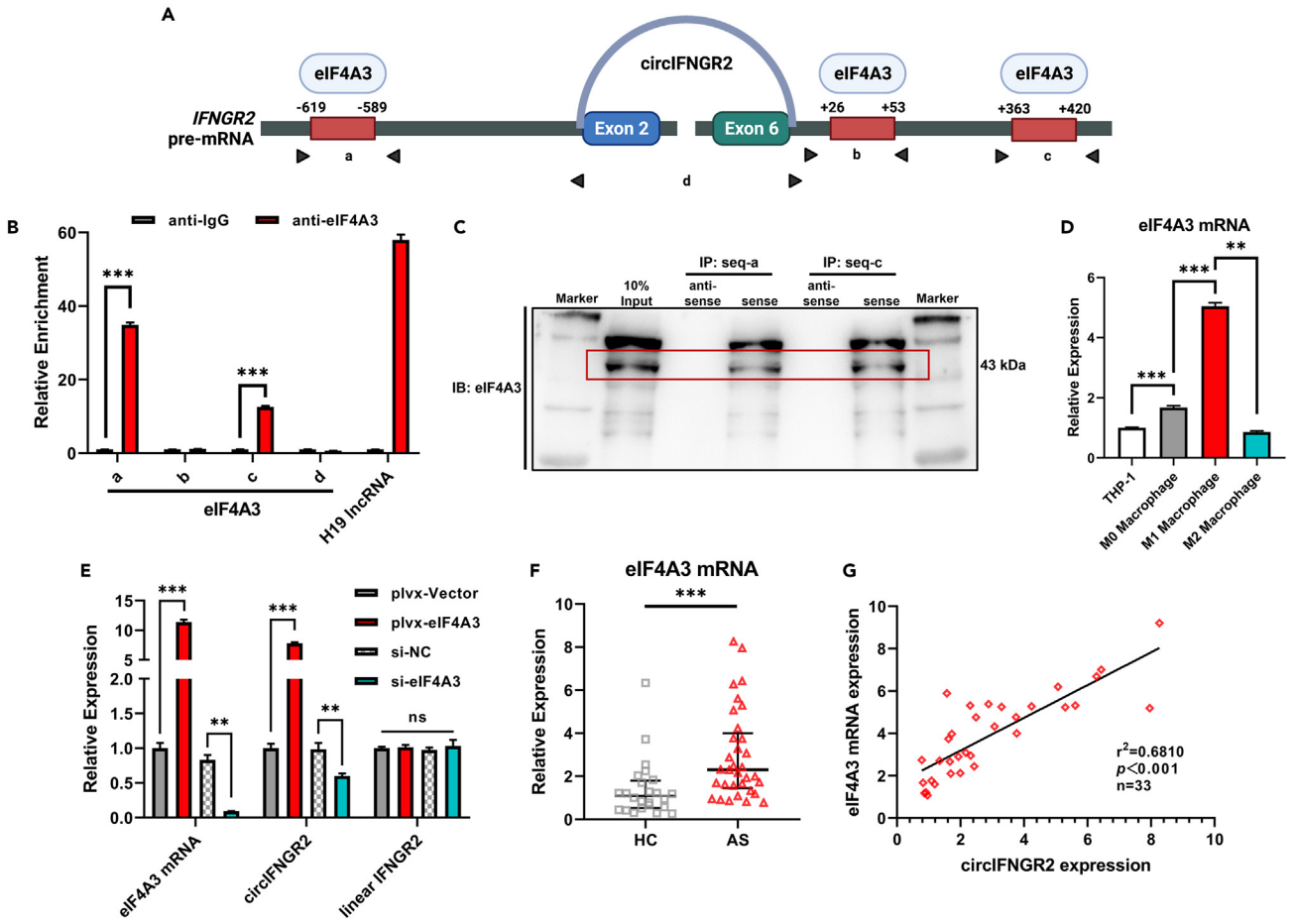

Figure 3. eIF4A3 regulated the expression of circIFNGR2

(A) The binding sites of eIF4A3 in the flanking sequences of the IFNGR2 pre-mRNA transcript were predicted by circInteractome.

(B) RIP assays for detection of the binding relationships among eIF4A3 and IFNGR2 pre-mRNA transcripts.

(C) Western Blot analysis for identification of the binding relationships among eIF4A3 and the flanking sequences of IFNGR2 pre-mRNA transcripts.

(D) qRT-PCR analysis of the expression level of eIF4A3 mRNA in THP-1 cells, M0 macrophages, M1 macrophages, and M2 macrophages.

(E) qRT-PCR analysis of the expression level of eIF4A3 mRNA, circIFNGR2, and linear IFNGR2 with or without overexpression and knockdown of eIF4A3.

(F) qRT-PCR analysis of the expression of circIFNGR2 in PBMCs from 24 healthy controls and 33 patients with AS.

(G) Correlation analysis of the expression levels of circIFNGR2 and eIF4A3 mRNA in PBMCs from patients with AS.

Data in B, D, and E are presented as mean ± SD, data in F are presented as median and quartiles. **: $p < 0.01$; ***: $p < 0.001$; ns: $p \geq 0.05$.

circIFNGR2 upregulated miR-939 (Figure 4K). On the contrary, neither overexpression nor knockdown of miR-939 altered the expression of circIFNGR2 or linear IFNGR2, indicating that the expression of circIFNGR2 was independent to miR-939 (Figure 4L). Since eIF4A3 was found to promote the expression of circIFNGR2, we also detected the expression levels of miR-939 in THP-1 cells with overexpression or knockdown of eIF4A3. Interestingly, miR-939 was downregulated in cells with overexpression of eIF4A3 but unchanged in cells with knockdown of eIF4A3 (Figure S4). In summary, results described previously implied that circIFNGR2 repressed the expression of miR-939 by serving as a sponge.

circIFNGR2 regulates iNOS/TNFα and macrophage polarization via miR-939

We screened the potential targets of miR-939 in TargetScan database and found that the 3′ UTR regions of iNOS and TNFα might have binding sites with miR-939 (Figure 5A). RAP assays using biotin-labeled probes targeted miR-939 showed that miR-939 could both bind to iNOS and TNFα (Figures 5B and 5C). To analyze the regulation of circIFNGR2/miR-939 on the expression of iNOS/TNFα and macrophage polarization, we conducted a series of rescue experiments in THP-1-derived macrophages with co-expression of circIFNGR2/miR-939. Firstly, EdU tests showed that miR-939 decreased cell proliferation and the promotion

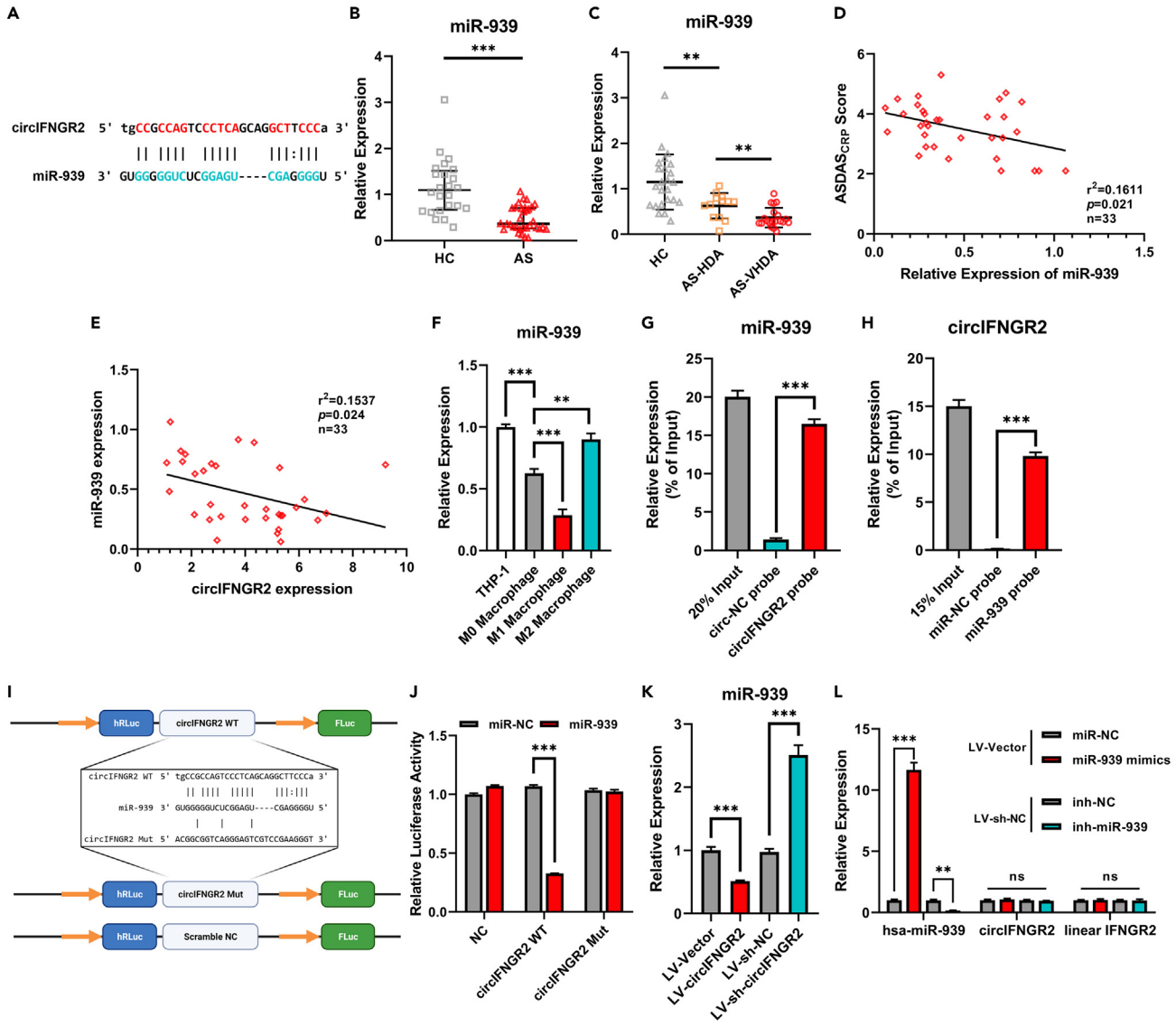

Figure 4. circIFNGR2 sponged and downregulated the expression of miR-939

(A) Binding sites of circIFNGR2 and miR-939 were predicted by TargetScan.

(B and C) qRT-PCR analysis of the expression of miR-939 in PBMCs from 24 healthy controls and 33 patients with AS including 13 patients with high disease activity (HDA, 2.1 ≤ ASDASCRP score < 3.5) and 20 patients with very high disease activity (VHDA, ASDASCRP score ≥ 3.5).

(D) Correlation analysis of $ASDAS_{CRP}$ score and the expression levels of miR-939 in PBMCs from patients with AS.

(E) Correlation analysis of the expression levels of miR-939 and circIFNGR2 in PBMCs from patients with AS.

(F) qRT-PCR analysis of the expression level of miR-939 in THP-1 cells, M0 macrophages, M1 macrophages, and M2 macrophages.

(G) qRT-PCR analysis of miR-939 in the immunoprecipitates of RAP assays using probes for circIFNGR2 or negative control.

(H) qRT-PCR analysis of circIFNGR2 in the immunoprecipitates of RAP assays using probes for miR-939 or negative control.

(I and J) Dual-luciferase reporter assay for validation of the binding between circIFNGR2 and miR-939.

(K) qRT-PCR analysis of the expression level of miR-939 in circIFNGR2 stably transfected THP-1 cells.

(L) qRT-PCR analysis of the expression level of miR-939, circIFNGR2, and linear IFNGR2 in THP-1 cells with overexpression or knockdown of miR-939.

Data in B and C are presented as median and quartiles, data in bar plots are presented as mean ± SD. **: $p < 0.01$; ***: $p < 0.001$.

of cell proliferation by circIFNGR2 was reversed by co-expression of miR-939 (Figures S5A and S5B). qRT-PCR and Western blot analysis revealed that overexpression of miR-939 rescued the positive regulatory effect of circIFNGR2 on iNOS, TNFα, CD86, and IL6 (Figures 5D, 5E and S5C). Flow cytometry analysis showed that in M1 macrophages, co-expression of circIFNGR2 and miR-939 led to decreased proportion of the $iNOS^{+}TNF\alpha^{+}$ cells compared to overexpression of circIFNGR2 only (Figures 5F, 5G, and S6). The results

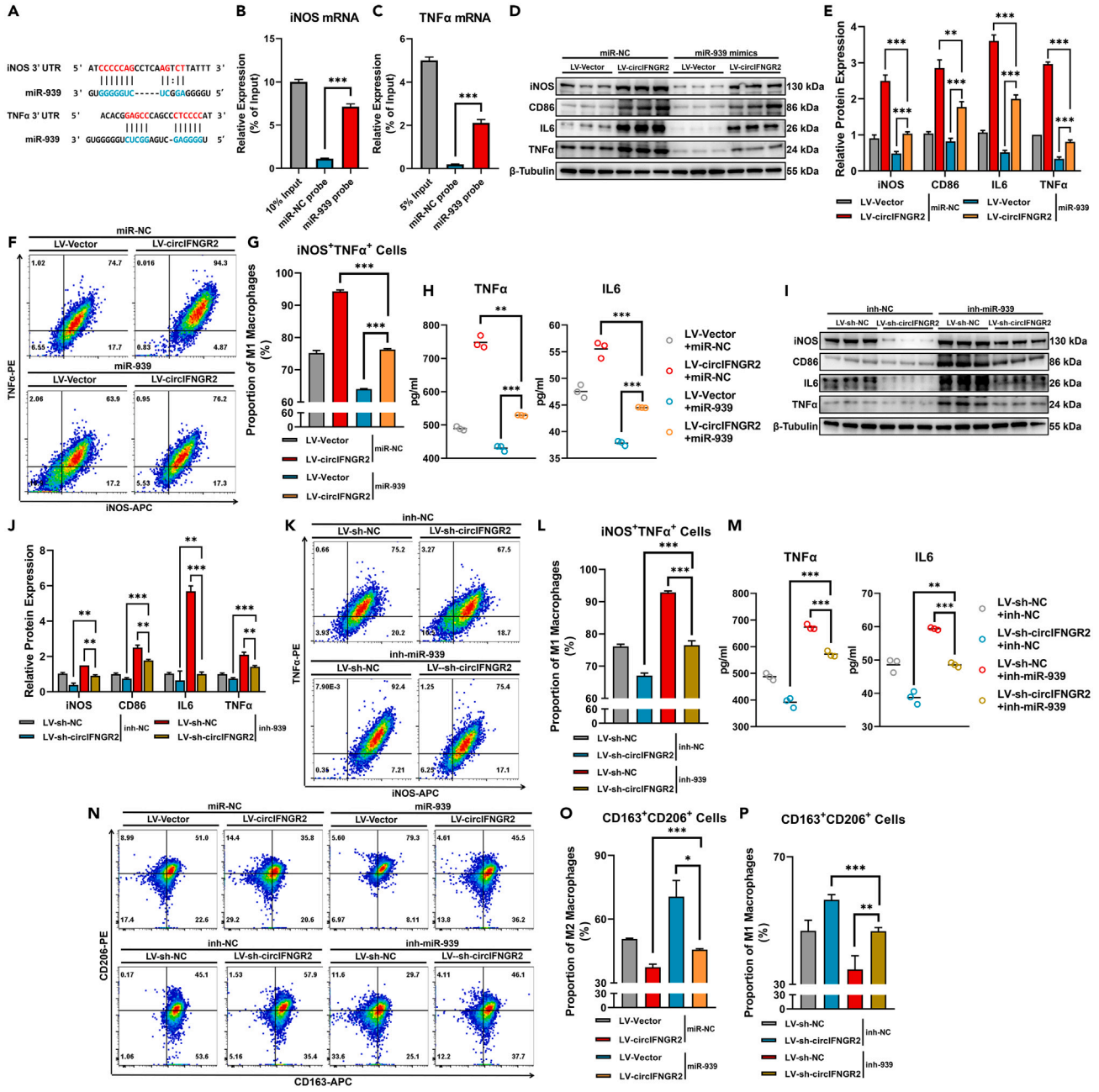

Figure 5. circIFNGR2 regulated the expression of iNOS/TNFα and M1/M2 macrophages polarization via miR-939

(A) Binding sites of circIFNGR2 and 3′ UTR regions of iNOS/TNFα mRNA were predicted by TargetScan.

(B and C) qRT-PCR analysis of iNOS/TNFα mRNA in the immunoprecipitates of RAP assays using probes for miR-939 or negative control.

(D and E) Western Blot analysis of relative protein expression of iNOS, CD86, IL6, and TNFα in THP-1-derived M1 macrophages with overexpression of circIFNGR2 and miR-939.

(F and G) Flow cytometry analysis of iNOS+TNFα+ cells in THP-1-derived M1 macrophages with overexpression of circIFNGR2 and miR-939.

(H) ELISA analysis of the secretion levels of TNFα and IL6 in THP-1-derived M1 macrophages with overexpression of circIFNGR2 and miR-939.

(I and J) Western Blot analysis of relative protein expression of iNOS, CD86, IL6, and TNFα in THP-1-derived M1 macrophages with knockdown of circIFNGR2 and miR-939.

(K and L) Flow cytometry analysis of iNOS+TNFα+ cells in THP-1-derived M1 macrophages with knockdown of circIFNGR2 and miR-939.

(M) ELISA analysis of the secretion levels of TNFα and IL6 in THP-1-derived M1 macrophages with knockdown of circIFNGR2 and miR-939.

(N–P) Flow cytometry analysis of iNOS+TNFα+ cells in THP-1-derived M2 macrophages with overexpression or knockdown of circIFNGR2 and miR-939.

Data in bar plots are presented as mean ± SD, data in scatterplots are supplemented with line of mean. *: $p < 0.05$; **: $p < 0.01$; ***: $p < 0.001$.

from ELISA assays also demonstrated that the upregulation of TNFα, IL6, IL1β, and IL23 was attenuated by co-expression of miR-939 (Figures 5H and S7A). Next, we used THP-1-derived macrophages with co-expression of sh-circIFNGR2 and miR-939 inhibitor. Data from qRT-PCR and Western blot analysis illustrated that knockdown of miR-939 restored the expression of iNOS, TNFα, CD86, and IL6 in M1 macrophages with knockdown of circIFNGR2 (Figures 5I, 5J, and S5D). Similarly, miR-939 inhibitor rescued the restraint of proportion of the $iNOS^{+}TNF\alpha^{+}$ cells caused by knockdown of circIFNGR2 (Figures 5K and 5L). Likewise, the suppressive influence of circIFNGR2 knockdown on pro-inflammatory cytokines (TNFα, IL6, IL1β, and IL23) was recovered by miR-939 inhibitor (Figures 5M and S7B). Additionally, in M2 macrophages, miR-939 mimics or inhibitors markedly reversed the decrease or increase of proportions of $CD163^{+}CD206^{+}$ cells induced by overexpression or knockdown of circIFNGR2, respectively (Figures 5N–5P). In conclusion, circIFNGR2 aggravated the expression of iNOS/TNFα and pro-inflammatory polarization by targeting miR-939.

circIFNGR2/miR-939 mediates the progression of inflammatory arthritis *in vivo*

To further investigate the functions of circIFNGR2/miR-939 *in vivo*, we established *in vivo* transfection of circIFNGR2/miR-939 in collagen-induced arthritis (CIA) mice as presented in Figure 6A. After the first immunization, the mice overexpressed with miR-939 exhibited remarkably less redness and swelling of hind paws than controls but restored by co-transfection with circIFNGR2 (Figure 6B). Notably, the clinical arthritis score also dramatically lower in the mice overexpressed with miR-939 than in the control group, while circIFNGR2 significantly reversed this reduction (Figure 6C). Through H&E staining and histological assessment of hind paws, we found that overexpression of miR-939 protected CIA mice from immune cells infiltration, synovial hyperplasia, bone erosion, and pannus formation of joints, which deteriorated when co-transfection with circIFNGR2 (Figures 6D and 6E). Subsequently, we conducted Safranin O-Fast Green staining to evaluate the cartilage damage of CIA mice. The results revealed that the structural damage of cartilage obviously mitigated in the mice with overexpression of miR-939 compared with controls. Consistently, the relief of cartilage damage by miR-939 was partially restored by co-transfection of circIFNGR2 (Figures 6F and 6G). To sum up, these findings illustrated that miR-939 attenuated the progression of inflammatory arthritis and could be reversed by circIFNGR2 *in vivo*.

DISCUSSION

Since the pathogenesis of AS remains unclarified, there is still lack of specific biomarkers for early diagnosis and treatment monitoring.[20] Due to the stability of circular structure and resistance to RNase R, circRNAs have the potential to be diagnostic and therapeutic molecular targets. Along with the developments of high-throughput RNA sequencing techniques, more and more differentially expressed circRNAs have been recognized in variety of diseases. Wang T et al.[21] have found the differential expression profiles in platelets samples collected from patients with AS. In our present study, we chose from our previous results of circRNA sequencing and identified the relatively high expression of circIFNGR2 with clinical significance. Mechanistically, eIF4A3-induced circIFNGR2 could promote the expression of iNOS/TNFα, augment M1 polarization and NF-κB pathways, while attenuate M2 polarization and Akt pathways by sponging miR-939.

CircRNAs were initially recognized as by-products of gene transcription without any function.[15] Nowadays, there are increasing evidences that functional circRNAs play vital roles in multiple diseases in various ways, particularly in the regulation of macrophage activation.[10] It has been previously reported that circANRIL promoted apoptosis of macrophages by activating p53 and protected patients from atherosclerosis.[22] Jiang F et al.[23] have explored that circ_0000518 ameliorated the progression of multiple sclerosis by binding to FUS protein, activating CaMKKβ/AMPK-PGC-1α pathways and M1 macrophage polarization, while restraining M2 macrophage polarization. It has been reported that NF-κB accelerated M1 polarization, while Akt reinforced M2 polarization.[24] Yang J et al.[13] have reported that circRNA_09505 could aggravate inflammation and joint damage in RA mice models by upregulating NF-κB pathways. Nevertheless, the roles of circRNA in macrophages and its underlying activating mechanisms were still unclear in AS. In the present study, we identified that circIFNGR2 was mainly located in $CD14^{+}$ cells in PBMCs and its expression levels elevated in M1 macrophages but decreased in M2 macrophages, indicating that circIFNGR2 might involve in the polarization of macrophages. Then, we found that overexpression of circIFNGR2 augmented cell proliferation, M1 polarization, activation of NF-κB pathways, and the secretion of pro-inflammatory cytokines. On the contrary, overexpression of circIFNGR2 inhibited M2 polarization as well as the activation of Akt pathways. Given that M1 macrophages mainly act as pro-inflammatory roles and M2 macrophages are broadly recognized as anti-inflammatory messenger, these findings suggested

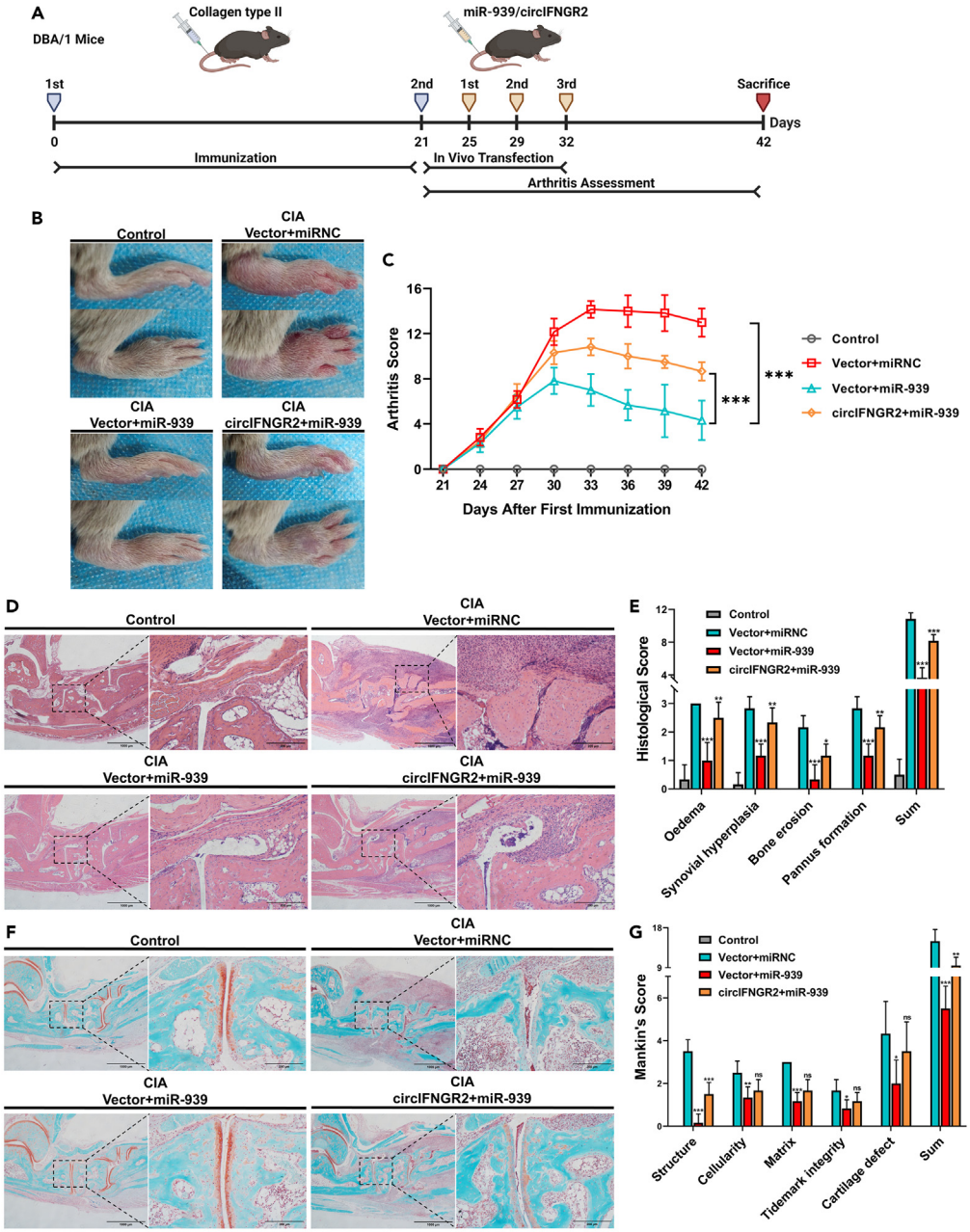

Figure 6. miR-939 ameliorated inflammatory arthritis and restored by circIFNGR2 *in vivo*

(A) Schematic illustration of experimental setup of CIA mouse model induction and transfection of miR-939 and circIFNGR2.

(B) Arthritis score of CIA mice with or without overexpression of miR-939 and circIFNGR2.

(C) Representative images of hind paws of CIA mice with or without overexpression of miR-939 and circIFNGR2.

(D and E) H&E staining and histological score of CIA mice with or without overexpression of miR-939 and circIFNGR2.

(F and G) Safranin O-Fast Green (SOFG) staining and Mankin's score of CIA mice with or without overexpression of miR-939 and circIFNGR2.

Data are presented as mean ± SD. *: $p < 0.05$; **: $p < 0.01$; ***: $p < 0.001$.

circIFNGR2 acts as a pro-inflammatory regulator in macrophage polarization. Nevertheless, M1 and M2 macrophages serve distinct functions in different stages of AS, with M2 macrophages playing roles in tissue repair in early-stage AS but involving in abnormal new bone formation in advanced AS. This suggests that circIFNGR2 may play stage-specific roles in the development of AS.

The biogenesis of circRNAs is regulated by flanking sequence including *cis*-elements and Alu short repeats, where RBPs could bind to.[25] Among these RBPs, eIF4A3 has been proved to bind to the downstream of circPRKAR1B and promote its expression in osteosarcoma.[26] Previous results from the research for glioblastoma indicated that eIF4A3 not only facilitated the biogenesis of circASAP1 but also correlated with disease status.[27] Our current study found that eIF4A3 could bind to both upstream and downstream flanking sequences of circIFNGR2, and enhanced the expression of circIFNGR2. Interestingly, we also found that the expression level of eIF4A3 was significantly upregulated in PBMCs samples from patients with AS, suggesting eIF4A3 might be also involved in the pathogenesis of AS. Surprisingly, alteration of eIF4A3 did not induce significant change on the expression levels of miR-939. The regulation of ncRNA biogenesis is known to be diverse and complex, suggesting that RBPs, such as eIF4A3, may not be the sole regulatory factor influencing the circIFNGR2/miR-939 axis. Furthermore, it is important to consider that when manipulating the expression of eIF4A3, either through overexpression or knockdown, there could be other regulatory mechanisms at play in the biogenesis of miR-939. These findings indicate that variables might exist in the regulatory effects through eIF4A3/circIFNGR2 to miR-939. Nevertheless, the comprehensive functional roles of eIF4A3 and circIFNGR2 in AS and other autoimmune diseases require further clarification.

Generally, cytoplasmic circRNAs acted as sponges for miRNAs and restored the inhibition of downstream genes.[28] We confirmed that circIFNGR2 was primarily located in cytoplasm of macrophages and could bind to miR-939. Previous reports revealed that miR-939 inhibited the expression of iNOS/TNFα by directly binding to 3′ UTR and abolished translations of inflammatory genes by interacting with NF-κB, indicating that miR-939 might play a vital role as an anti-inflammatory mediator.[29–32] In our present study, we evaluated the expression of miR-939 in PBMCs and found that the expression levels of miR-939 were negatively correlated with disease activity score of AS and the expression levels of circIFNGR2. Then, we verified that circIFNGR2 sponged and suppress miR-939, while miR-939 did not interfere the expression of circIFNGR2 and its host gene, IFNGR2. Moreover, *in vitro* rescue assays showed that miR-939 reversed the pro-inflammatory effects of circIFNGR2 on cell proliferation, M1/M2 polarization, and cytokines secretion. Surprisingly, *in vivo* experiments demonstrated that miR-939 significantly ameliorated the clinical appearance, immune cells infiltration, and bone and cartilage damage of the inflammatory arthritis in CIA mice, which was partially resumed by circIFNGR2. These results illustrate the important roles of AS-specific circIFNGR2/miR-939 in regulation of macrophage-related inflammation.

Collectively, our study identified that circIFNGR2 was upregulated in PBMCs from patients with AS and correlated with disease activities. Specifically, eIF4A3-induced circIFNGR2 acted as a sponge for miR-939 and therefore aggravated pro-inflammatory activation of macrophage in AS-associated inflammation. This study may broaden our understandings of AS pathogenesis and provides a potential therapeutic strategy targeting circINFGR2/miR-939 in clinical practice for AS.

Limitations of the study

This study has potential limitations. Although the functionality of circIFNGR2 was confirmed in our current research, it is important to note that the initial assessment of differentially expressed circRNAs in AS was based on a small sample size, which could introduce biases in the identification of clinically significant circRNAs. Additionally, our study only focused on circIFNGR2 and its association with bone and cartilage destruction in inflammatory arthritis, which were relative early stage of AS pathophysiological processes, while the inappropriate tissue repair and abnormal osteogenesis were not fully covered in current study. Furthermore, due to the lack of specific mouse models that fully replicate the complex pathogenesis of AS, we utilized the CIA model as a substitute in our *in vivo* experiments. This choice may restrict our ability to fully elucidate the AS-specific roles of circIFNGR2.

STAR★METHODS

Detailed methods are provided in the online version of this paper and include the following:

- KEY RESOURCES TABLE
- RESOURCE AVAILABILITY
  - Lead contact
  - Materials availability
  - Data and code availability
- EXPERIMENTAL MODE AND STUDY PARTICIPANT DETAILS
  - Patients and samples

SUPPLEMENTAL INFORMATION

Supplemental information can be found online at https://doi.org/10.1016/j.isci.2023.107325.

ACKNOWLEDGMENTS

This work was supported by grants from Guangdong Basic and Applied Basic Research Foundation (grant No. 2022A1515111081), Basic and Application Base Research Project of Guangzhou Basic Research Plan in 2022 (grant No. 202201011436), Natural Science Foundation of Jiangxi Province (grant No. 20224BAB206031), Ganzhou Science and Technology Innovation Talent Project (grant No. GZKJ20220638), Clinical Research Startup Program of Southern Medical University by the High-level University Construction Funding of Guangdong Provincial Department of Education (grant No. LC2019ZD022), the President Foundation of Nanfang Hospital, Southern Medical University (grant No. 2020C010, 2020C023 and 2022B026), Clinical Research Program of Nanfang Hospital, Southern Medical University (grant No. 2018CR001 and 2020CR028), and the National Natural Science Foundation of China (grant No. 81872557).

AUTHOR CONTRIBUTIONS

M.S., X.W., and J.G. wrote this manuscript, conducted *in vitro* and *in vivo* experiments, analyzed the data, and assembled the figures; W.J. performed Western blot and qRT-PCR analysis; T.A., T.W., Z.C., and W.L. collected clinical samples and analyzed the data; E.B. and Z.S. contributed to the design of this research; C.Z. and J.X. designed this study, edited this manuscripts and act as co-corresponding authors. C.Z. is the lead contact of this manuscript. All authors read and approved the final version of the manuscript.

DECLARATION OF INTERESTS

The authors have declared that no conflict of interest exists.

Received: April 6, 2023
Revised: June 4, 2023
Accepted: July 5, 2023
Published: July 10, 2023

REFERENCES

1. Taurog, J.D., Chhabra, A., and Colbert, R.A. (2016). Ankylosing Spondylitis and axial Spondyloarthritis. N. Engl. J. Med. *374*, 2563–2574. https://doi.org/10.1056/NEJMra1406182.

2. Mauro, D., Thomas, R., Guggino, G., Lories, R., Brown, M.A., and Ciccia, F. (2021). Ankylosing spondylitis: an autoimmune or autoinflammatory disease? Nat. Rev. Rheumatol. *17*, 387–404. https://doi.org/10.1038/s41584-021-00625-y.

3. Ranganathan, V., Gracey, E., Brown, M.A., Inman, R.D., and Haroon, N. (2017). Pathogenesis of ankylosing spondylitis - recent advances and future directions. Nat. Rev. Rheumatol. *13*, 359–367. https://doi.org/10.1038/nrrheum.2017.56.

4. Ma, W.T., Gao, F., Gu, K., and Chen, D.K. (2019). The role of monocytes and macrophages in autoimmune diseases: a comprehensive review. Front. Immunol. *10*, 1140. https://doi.org/10.3389/fimmu.2019.01140.

5. Funes, S.C., Rios, M., Escobar-Vera, J., and Kalergis, A.M. (2018). Implications of macrophage polarization in autoimmunity. Immunology *154*, 186–195. https://doi.org/10.1111/imm.12910.

6. Song, M., Gao, J., Yan, T., Bi, E., An, T., Wang, X., Jiang, W., Wang, T., Chen, Z., Shi, Z., et al. (2021). Hsa_circ_0000652 aggravates

inflammation by activation of macrophages and enhancement of OX40/OX40L interaction in Ankylosing Spondylitis. Front. Cell Dev. Biol. *9*, 737599. https://doi.org/10.3389/fcell.2021.737599.

7. Wilusz, J.E. (2018). A 360 degrees view of circular RNAs: from biogenesis to functions. Wiley Interdiscip Rev RNA *9*, e1478. https://doi.org/10.1002/wrna.1478.

8. Guo, G., Wang, H., Ye, L., Shi, X., Yan, K., Lin, K., Huang, Q., Li, B., Lin, Q., Zhu, L., et al. (2019). Hsa_circ_0000479 as a novel diagnostic biomarker of systemic Lupus Erythematosus. Front. Immunol. *10*, 2281. https://doi.org/10.3389/fimmu.2019.02281.

9. Li, B., Li, N., Zhang, L., Li, K., Xie, Y., Xue, M., and Zheng, Z. (2018). Hsa_circ_0001859 regulates ATF2 expression by functioning as an MiR-204/211 sponge in human rheumatoid arthritis. J. Immunol. Res. *2018*, 9412387. https://doi.org/10.1155/2018/9412387.

10. Zhou, Z., Sun, B., Huang, S., and Zhao, L. (2019). Roles of circular RNAs in immune regulation and autoimmune diseases. Cell Death Dis. *10*, 503. https://doi.org/10.1038/s41419-019-1744-5.

11. Chen, X., Yang, T., Wang, W., Xi, W., Zhang, T., Li, Q., Yang, A., and Wang, T. (2019). Circular RNAs in immune responses and immune diseases. Theranostics *9*, 588–607. https://doi.org/10.7150/thno.29678.

12. Song, H., Yang, Y., Sun, Y., Wei, G., Zheng, H., Chen, Y., Cai, D., Li, C., Ma, Y., Lin, Z., et al. (2022). Circular RNA Cdyl promotes abdominal aortic aneurysm formation by inducing M1 macrophage polarization and M1-type inflammation. Mol. Ther. *30*, 915–931. https://doi.org/10.1016/j.ymthe.2021.09.017.

13. Yang, J., Cheng, M., Gu, B., Wang, J., Yan, S., and Xu, D. (2020). CircRNA_09505 aggravates inflammation and joint damage in collagen-induced arthritis mice via miR-6089/AKT1/NF-kappaB axis. Cell Death Dis. *11*, 833. https://doi.org/10.1038/s41419-020-03038-z.

14. Zhang, C., Han, X., Yang, L., Fu, J., Sun, C., Huang, S., Xiao, W., Gao, Y., Liang, Q., Wang, X., et al. (2020). Circular RNA circPPM1F modulates M1 macrophage activation and pancreatic islet inflammation in type 1 diabetes mellitus. Theranostics *10*, 10908–10924. https://doi.org/10.7150/thno.48264.

15. Kristensen, L.S., Andersen, M.S., Stagsted, L.V.W., Ebbesen, K.K., Hansen, T.B., and Kjems, J. (2019). The biogenesis, biology and characterization of circular RNAs. Nat. Rev. Genet. *20*, 675–691. https://doi.org/10.1038/s41576-019-0158-7.

16. Yang, M., Hu, H., Wu, S., Ding, J., Yin, B., Huang, B., Li, F., Guo, X., and Han, L. (2022). EIF4A3-regulated circ_0087429 can reverse EMT and inhibit the progression of cervical cancer via miR-5003-3p-dependent upregulation of OGN expression. J. Exp. Clin. Cancer Res. *41*, 165. https://doi.org/10.1186/s13046-022-02368-4.

17. Zhao, J., Jiang, Y., Chen, L., Ma, Y., Zhang, H., Zhou, J., Li, H., and Jing, Z. (2021). The EIF4A3/CASC2/RORA feedback loop regulates the aggressive phenotype in glioblastomas. Front. Oncol. *11*, 699933. https://doi.org/10.3389/fonc.2021.699933.

18. Wang, X., Liu, S., Xu, B., Liu, Y., Kong, P., Li, C., and Li, B. (2021). circ-SIRT1 promotes colorectal cancer proliferation and EMT by recruiting and binding to eIF4A3. Anal. Cell Pathol. *2021*, 5739769. https://doi.org/10.1155/2021/5739769.

19. Conn, S.J., Pillman, K.A., Toubia, J., Conn, V.M., Salmanidis, M., Phillips, C.A., Roslan, S., Schreiber, A.W., Gregory, P.A., and Goodall, G.J. (2015). The RNA binding protein quaking regulates formation of circRNAs. Cell *160*, 1125–1134. https://doi.org/10.1016/j.cell.2015.02.014.

20. Ward, M.M., Deodhar, A., Gensler, L.S., Dubreuil, M., Yu, D., Khan, M.A., Haroon, N., Borenstein, D., Wang, R., Biehl, A., et al. (2019). 2019 update of the American college of rheumatology/Spondylitis association of America/Spondyloarthritis research and treatment network recommendations for the treatment of ankylosing spondylitis and nonradiographic axial spondyloarthritis. Arthritis Rheumatol. *71*, 1599–1613. https://doi.org/10.1002/art.41042.

21. Wang, T., Meng, S., Chen, P., Wei, L., Liu, C., Tang, D., Liu, D., Jiang, Z., and Hong, X. (2021). Comprehensive analysis of differentially expressed mRNA and circRNA in Ankylosing spondylitis patients' platelets. Exp. Cell Res. *409*, 112895. https://doi.org/10.1016/j.yexcr.2021.112895.

22. Holdt, L.M., Stahringer, A., Sass, K., Pichler, G., Kulak, N.A., Wilfert, W., Kohlmaier, A., Herbst, A., Northoff, B.H., Nicolaou, A., et al. (2016). Circular non-coding RNA ANRIL modulates ribosomal RNA maturation and atherosclerosis in humans. Nat. Commun. *7*, 12429. https://doi.org/10.1038/ncomms12429.

23. Jiang, F., Liu, X., Cui, X., Hu, J., Wang, L., Xue, F., Guo, S., and Wang, X. (2022). Circ_0000518 promotes macrophage/microglia M1 polarization via the FUS/CaMKKbeta/AMPK pathway to aggravate multiple sclerosis. Neuroscience *490*, 131–143. https://doi.org/10.1016/j.neuroscience.2021.12.012.

24. Yunna, C., Mengru, H., Lei, W., and Weidong, C. (2020). Macrophage M1/M2 polarization. Eur. J. Pharmacol. *877*, 173090. https://doi.org/10.1016/j.ejphar.2020.173090.

25. Chen, L.L. (2020). The expanding regulatory mechanisms and cellular functions of circular RNAs. Nat. Rev. Mol. Cell Biol. *21*, 475–490. https://doi.org/10.1038/s41580-020-0243-y.

26. Feng, Z.H., Zheng, L., Yao, T., Tao, S.Y., Wei, X.A., Zheng, Z.Y., Zheng, B.J., Zhang, X.Y., Huang, B., Liu, J.H., et al. (2021). EIF4A3-induced circular RNA PRKAR1B promotes osteosarcoma progression by miR-361-3p-mediated induction of FZD4 expression. Cell Death Dis. *12*, 1025. https://doi.org/10.1038/s41419-021-04339-7.

27. Wei, Y., Lu, C., Zhou, P., Zhao, L., Lyu, X., Yin, J., Shi, Z., and You, Y. (2021). EIF4A3-induced circular RNA ASAP1 promotes tumorigenesis and temozolomide resistance of glioblastoma via NRAS/MEK1/ERK1-2 signaling. Neuro Oncol. *23*, 611–624. https://doi.org/10.1093/neuonc/noaa214.

28. Hansen, T.B., Jensen, T.I., Clausen, B.H., Bramsen, J.B., Finsen, B., Damgaard, C.K., and Kjems, J. (2013). Natural RNA circles function as efficient microRNA sponges. Nature *495*, 384–388. https://doi.org/10.1038/nature11993.

29. Lin, Y., Zhou, Z., Xie, L., Huang, Y., Qiu, Z., Ye, L., and Cui, C. (2022). Effects of miR-939 and miR-376A on ulcerative colitis using a decoy strategy to inhibit NF-kappaB and NFAT expression. Eur. J. Histochem. *66*, 3316. https://doi.org/10.4081/ejh.2022.3316.

30. Ramanathan, S., Shenoda, B.B., Lin, Z., Alexander, G.M., Huppert, A., Sacan, A., and Ajit, S.K. (2019). Inflammation potentiates miR-939 expression and packaging into small extracellular vesicles. J. Extracell. Vesicles *8*, 1650595. https://doi.org/10.1080/20013078.2019.1650595.

31. McDonald, M.K., Ramanathan, S., Touati, A., Zhou, Y., Thanawala, R.U., Alexander, G.M., Sacan, A., and Ajit, S.K. (2016). Regulation of proinflammatory genes by the circulating microRNA hsa-miR-939. Sci. Rep. *6*, 30976. https://doi.org/10.1038/srep30976.

32. Guo, Z., Shao, L., Zheng, L., Du, Q., Li, P., John, B., and Geller, D.A. (2012). miRNA-939 regulates human inducible nitric oxide synthase posttranscriptional gene expression in human hepatocytes. Proc. Natl. Acad. Sci. USA *109*, 5826–5831. https://doi.org/10.1073/pnas.1118118109.

33. Brand, D.D., Latham, K.A., and Rosloniec, E.F. (2007). Collagen-induced arthritis. Nat. Protoc. *2*, 1269–1275. https://doi.org/10.1038/nprot.2007.173.

34. Liu, R., Tao, E., Yu, S., Liu, B., Dai, L., Yu, L., Xiong, Y., Fu, R., Lei, L., and Lai, X. (2016). The suppressive effects of the petroleum ether fraction from Atractylodes lancea (Thunb.) DC. On a Collagen-Induced Arthritis Model. Phytother Res. *30*, 1672–1679. https://doi.org/10.1002/ptr.5671.

35. Salo, P.T., Hogervorst, T., Seerattan, R.A., Rucker, D., and Bray, R.C. (2002). Selective joint denervation promotes knee osteoarthritis in the aging rat. J. Orthop. Res. *20*, 1256–1264. https://doi.org/10.1016/S0736-0266(02)00045-1.

STAR★METHODS

KEY RESOURCES TABLE

REAGENT or RESOURCE	SOURCE	IDENTIFIER
Antibodies		
Rabbit monoclonal anti-iNOS	Abcam	Cat# ab178945; RRID: AB_2861417
Rabbit polyclonal anti-TNFα	proteintech	Cat# 17590-1-AP; RRID: AB_2271853
Rabbit polyclonal anti-IL1β	Bioss	Cat# bs-0812R; RRID: AB_10855142
Rabbit monoclonal anti-IL6	Abcam	Cat# ab233706; RRID: AB_2889391
Rabbit polyclonal anti-CD86	Bioss	Cat# bs-1035R; RRID: AB_10856252
Rabbit polyclonal anti-p65	Beyotime	Cat# AF0246; RRID: AB_2923151
Rabbit polyclonal anti-phospho-p65	Beyotime	Cat# AF5875;
Rabbit monoclonal anti-Iκκα/β	Beyotime	Cat# AF5839
Rabbit polyclonal anti-Akt	Abmart	Cat# T55561; RRID: AB_2936969
Rabbit polyclonal anti-phospho-Akt	Abmart	Cat# TA0016
Rabbit polyclonal anti-mTOR	Abmart	Cat# T55306; RRID: AB_2936905
Rabbit polyclonal anti-phospho-mTOR	Abmart	Cat# T56571, RRID: AB_2936395
Rabbit polyclonal anti-eIF4A3	Bioss	Cat# bs-14548R
Rabbit polyclonal anti-Histone H3	Bioss	Cat# bs-0349R, RRID: AB_10857220
Mouse polyclonal anti-β-Tubulin	Abmart	Cat# MA9126
HRP-conjugated Affinipure Goat Anti-Rabbit IgG(H + L)	proteintech	Cat# SA00001-2, RRID: AB_2722564
HRP-conjugated Affinipure Goat Anti-Mouse IgG(H + L)	proteintech	Cat# SA00001-1, RRID: AB_2722565
APC monoclonal anti-human CD163	BioLegend	Cat# 326510, RRID: AB_2564015
PE monoclonal anti-human CD206	BioLegend	Cat# 321106, RRID: AB_571911
APC monoclonal anti-Nos2 (iNOS)	BioLegend	Cat# 696808
PE monoclonal anti-human TNF-alpha	BioLegend	Cat# 502909, RRID: AB_315261
Bacterial and virus strains		
plv-cir-cmv-hsa_circ_0002660-ef1-gfp-puro	IGEbio	N/A
plv-cir-cmv-mcs-ef1-gfp-puro	IGEbio	N/A
pLKO.1-U6-hsa_circ_0002660-sh1-EF1a-copGFP-T2A-puro	IGEbio	N/A
pLKO.1-U6-EF1a-copGFP-T2A-puro	IGEbio	N/A
plvx-XhoI-eif4a3-BamHI-amp-puro	tsingke	N/A
plvx-XhoI-BamHI-amp-puro	tsingke	N/A
Chemicals, peptides, and recombinant proteins		
penicillin/streptomycin solution	Gibco	Cat# 10378016
β-Mercaptoethanol	Solarbio	Cat# M8211
phorbol 12-myristate 13-acetate	Solarbio	Cat# P6741
Recombinant human IFNγ	Prospec	Cat# CYT-206
lipopolysaccharides	Solarbio	Cat# L8880
Recombinant human IL4	Prospec	Cat# CYT-211
Recombinant human IL13	Prospec	Cat# CYT-446
bovine type II collagen	Chondrex	Cat# 20022
complete Freund's adjuvant	Chondrex	Cat# 7023

(*Continued on next page*)

Continued

REAGENT or RESOURCE	SOURCE	IDENTIFIER
incomplete Freund's adjuvant	Chondrex	Cat# 7002
EntransterTM - *in vivo*	Engreen	Cat# 18668-11-2
DEPC water	Beyotime	Cat# R0022
TRIzol reagent	Invitrogen	Cat# 15596026
Hieff qPCR SYBR Green Master Mix	Yeasen	Cat# 11202ES
Lipo8000 Transfection Reagent	Beyotime	Cat# C0533
polybrene	Beyotime	Cat# C0351
RNase R	Epicenter	Cat# RNR07250
RIPA Lysis Buffer	Beyotime	Cat# P0013
Protease and phosphatase inhibitor	Beyotime	Cat# P1048
4-15% SDS-PAGE pre-cast gels	Beyotime	Cat# P0520
QuickBlock™ Blocking Buffer for Western Blot	Beyotime	Cat# P0252
Critical commercial assays		
PARIS kit	Life Technologies	Cat# AM1921
SteadyPure Universal Genomic DNA Extraction Kit	Accurate Biology	Cat# AG21010
BeyoClick EdU-555 kit	Beyotime	Cat# C0075
Nuclear and Cytoplasmic Protein Extraction Kit	Beyotime	Cat# P0028
enhanced BCA kit	Beyotime	Cat# P0010
BeyoECL kit	Beyotime	Cat# P0018
Human TNF alpha ELISA kit	MEIMIAN	Cat# MM-0122H1
Human IL6 ELISA Kit	MEIMIAN	Cat# MM-0049H1
Human IL1β ELISA Kit	MEIMIAN	Cat# MM-0181H1
Human IL23 ELISA Kit	MEIMIAN	Cat# MM-0196H2
Luc-pair Duo-Luciferase HS assay kit	GeneCopoeia	Cat# ZX001
RNA Antisense Purification Kit	Bersinbio	Cat# Bes5103
RNA Immunoprecipitation Kit	Bersinbio	Cat# Bes5101
Experimental models: Cell lines		
THP-1	iCell Bioscience	Cat# iCell-h213
HEK293T	iCell Bioscience	Cat# iCell-h237
Experimental models: Organisms/strains		
DBA/1J mice	Gempharmatech	Cat# N000219
Oligonucleotides		
circIFNGR2 primer – forward: ACTCCACCAAGCATCCCATT; reverse: GGCCGTGAACCATTTACTGT	tsingke	N/A
IFNGR2 primer – forward: AGAGTGTGACTTCACTGCCG; reverse: AACCAAGGCATTGTCACCCA	tsingke	N/A
β-Actin primer – forward: CATGTACGTTGCTATCCAGGC; reverse: CTCCTTAATGTCACGCACGAT	tsingke	N/A
GAPDH primer – forward: GGAGCGAGATCCCTCCAAAAT; reverse: GGCTGTTGTCATACTTCTCATGG	tsingke	N/A

(*Continued on next page*)

Continued

REAGENT or RESOURCE	SOURCE	IDENTIFIER
CD86 primer – forward: CTGCTCATCTATACACGGTTACC; reverse: GGAAACGTCGTACAGTTCTGTG	tsingke	N/A
IL6 primer – forward: AGTCCTGATCCAGTTCCTGC; reverse: CTACATTTGCCGAAGAGCCC	tsingke	N/A
iNOS primer – forward: CGCATGACCTTGGTGTTTGG; reverse: CATAGACCTTGGGCTTGCCA	tsingke	N/A
TNFα primer – forward: CCTCTCTCTAATCAGCCCTCTG; reverse: GAGGACCTGGGAGTAGATGAG	tsingke	N/A
eIF4A3 primer – forward: GGCACAGGAAAAACAGCCACCT; reverse: TGTAGTCACCGAGAGCAAGCAG	tsingke	N/A
lncH19 primer – forward: GCACCTTGGACATCTGGAGT; reverse: TTCTTTCCAGCCCTAGCTCA	tsingke	N/A
Seq-a in RIP assay primer – forward: ACGACAACTCTGATGGTGCC; reverse: AATCAGGTACGCAAAGCCCA	tsingke	N/A
Seq-b in RIP assay primer – forward: AGAAGAGGTACGTGTGCACA; reverse: AATCGCTTGAACCTGGGAGA	tsingke	N/A
Seq-c in RIP assay primer – forward: GGCAACCCCTAAGAGTGCAG; reverse: ACCCCATACCATTTGTAACCCAA	tsingke	N/A
miR-939 mimic: UGGGGAGCUGAGGCUCUGGGGGUG	RIBOBIO	N/A
miR-939 inhibitor: CACCCCCAGAGCCUCAGCUCCCCA	RIBOBIO	N/A
sh-circIFNGR2: CCGGACAGATAGAAGAG ACCCTCTTCTCGAGAAGAGGGTCTCTTCT ATCTGTTTTTTGAATT	IGEbio	N/A
si-eIF4A3 sense: CGAGCAAUCAAGCAGAUCATT; anti-sense: UGAUCUGCUUGAUUGCUCGTT	tsingke	N/A
circIFNGR2 RAP probe: AGGGTCTCTTC TATCTGTAA+AAAGAGGGTCTCTTCTATCT	RIBOBIO	N/A
miR-939 RAP probe: UGGGGAGC+UGAGGCUC+UGGGGGUG	RIBOBIO	N/A
Seq-a RAP anti-sense probe: GCACCATCAGAGTTGTCGTC	RIBOBIO	N/A
Seq-c RAP anti-sense probe: GTAACCCAAATCTCTGTGTC	RIBOBIO	N/A
Recombinant DNA		
pEZX-MT06 luciferase reporter vectors	GeneCopoeia	N/A
psPAX2	IGEbio	N/A
pMD2.G	IGEbio	N/A

(*Continued on next page*)

Continued

REAGENT or RESOURCE	SOURCE	IDENTIFIER
Software and algorithms		
FlowJo	Tree Star	N/A
GraphPad Prism 8	GraphPad Software	N/A

RESOURCE AVAILABILITY

Lead contact

Further information and requests for resources and reagents should be directed to and will be fulfilled by the lead contact, Chao Zhang (super1998@smu.edu.cn).

Materials availability

Further information and requests for resources and reagents should be directed to and will be fulfilled by the lead contact.

Data and code availability

- All data reported in this paper will be shared by the lead contact upon request.
- This paper does not report original code.
- Any additional information required to reanalyze the data reported in this paper is available from the lead contact upon request.

EXPERIMENTAL MODE AND STUDY PARTICIPANT DETAILS

Patients and samples

This study involved 33 patients with AS and 24 healthy controls at NanFang Hospital, Southern Medical University, Guangzhou, China. All involved AS patients fulfilled the inclusion and exclusion criteria of our ongoing clinical research (NCT04077957), which defined as mild to moderate AS with active inflammatory status and no need for surgical therapy. All persons involved in our study were Han Chinese. The demographical and clinical characteristics of involved AS patients were listed in Table S1. Peripheral blood samples of involved AS patients were collected before any medicine or other therapeutic measures applied. PBMCs were collected from peripheral blood using lymphocyte separation medium (Solarbio, Beijing, China) following the manufacturer's protocols. Primary $CD14^+/CD14^-$ cells were separated by MojoSort Human CD14 Selection Kit (BioLegend, CA, USA) according to the manufacturer's instructions. All patients and healthy controls signed the informed consent forms. This study was approved by Medical Ethics committee of NanFang Hospital of Southern Medical University.

Cell culture

The human THP-1 and HEK293T cell lines were obtained from the iCell Bioscience Inc. (Shanghai, China). THP-1 cells were cultured in RPMI-1640 medium (Gibco, MD, USA) supplemented with 15% fetal bovine serum (FBS, Gibco, MD, USA), 1% penicillin/streptomycin solution (Gibco, MD, USA) and 50 μM β-Mercaptoethanol (Solarbio, Beijing, China) in a humidified cell incubator with 5% CO_2 at 37°C. 293T cells were grown in Dulbecco's modified Eagle's medium with high glucose (DMEM, Gibco, MD, USA) with 10% FBS and 1% penicillin/streptomycin. For M0 macrophage differentiation, THP-1 cells were treated with 50 ng/mL phorbol 12-myristate 13-acetate (PMA, Solarbio, Beijing, China) for 24 h. For M1 polarization, THP1-derived M0 macrophages were then treated with 20 ng/mL IFNγ (Prospec, NZ, Israel) and 100 ng/mL lipopolysaccharides (LPS, Solarbio, Beijing, China) for another 48 h. For M2 polarization, THP1-derived M0 macrophages were treated with 20 ng/mL IL4 and 5 ng/mL IL13 (Prospec, NZ, Israel) for 48 h.

Animal models

Male DBA/1J mice aged 8 weeks were obtained from Gempharmatech Co., Ltd (Jiangsu, China) and kept in SPF grade environment. All *in vivo* experiments were conducted according to the protocols approved by the Institutional Animal Care and Use Committee of Nanfang hospital, Southern Medical University. For indction of collagen-induced arthritis, 100 μL bovine type II collagen (Chondrex, WA, USA) emulsified in

complete Freund's adjuvant (Chondrex, WA, USA) was subcutaneously injected to the base of tail vein of each mouse on day 0. On day 21 from the first immunization, boost injection of 100 μL bovine type II collagen emulsified in incomplete Freund's adjuvant (Chondrex, WA, USA) was conducted. The mice in control group (n = 6) were injected with saline at equal volume on each time. After the first immunization, CIA mice were randomly divided into 3 groups with n = 6 in each group: Vector+miRNC, Vector+miR939 and circIFNGR2+miR939. Plasmids containing empty vector or circIFNGR2 and miR-939 mimics or control sequences were diluted with Entranster - *in vivo* (Engreen, Beijing, China) and DEPC water (Beyotime, Beijing, China) and injected intravenously in day 25, 29 and 32. Arthritis Score was used for monitoring the clinical appearance of CIA mice every 3 days after the first immunization. This scoring system categorized the severity of arthritis as follows: a score of 0 indicated no evidence of erythema and swelling; a score of 1 denoted erythema and mild swelling confined to the tarsals or ankle joint; a score of 2 represented erythema and mild swelling extending from the ankle to the tarsals; a score of 3 indicated erythema and moderate swelling extending from the ankle to metatarsal joints; and finally, a score of 4 indicated erythema and severe swelling encompassing the ankle, foot, and digits, or the presence of limb ankylosis.[33]

Mice were sacrificed on day 42, and hind paw joints were collected, fixed in 4% paraformaldehyde, decalcificated and embedded in paraffin for histological analysis. hematoxylin and eosin (H&E) and Safranin O - Fast Green (SOFG) staining were used for evaluation of histologic changes in each group of mice. In H&E staining, histological score consisting of 4 dimensions with oedema (0–4), synovial hyperplasia (0–4), bone erosion (0–4) and pannus formation (0–4) was used for comprehensive arthritis assessment.[34] To evaluate cartilage damage, a modified Mankin's Score containing 5 dimensions including structure (0–6), cellularity (0–4), matrix staining (0–4), tidemark integrity (0–3) and cartilage defects (0–16) was applied in SOFG staining.[35]

METHODS DETAILS

RNA and genomic DNA extraction and quantitative real-time PCR (qRT-PCR)

TRIzol reagent (Invitrogen, CA, USA) was used for the extraction of total RNA from PBMCs and cultured cells following the manufacturer's instructions. The nuclear and cytoplasmic RNA and genomic DNA (gDNA) was extracted using PARIS kit (Life Technologies, CA, USA) and SteadyPure Universal Genomic DNA Extraction Kit (Accurate Biology, Hunan, China) respectively. Reverse transcriptions for mRNA, circRNA and miRNA analysis were conducted as previous described.[6] Hieff qPCR SYBR Green Master Mix (Yeasen Biotechnology, Shanghai, China) was used for qRT-PCR reactions. All results from qRT-PCR were detected by QuantStudio 3 (Applied Biosystems, CA, USA). *U6*, *GAPDH* and *β-Actin* were used as endogenous controls. The relative gene expression was calculated by the comparative Ct ($2^{-\Delta\Delta CT}$) method. All reactions were repeated in triplicate.

Cell transfection

Lentivirus was used for construction of circIFNGR2 stably-expression THP-1 cells previous described.[6] Briefly, the plasmids containing the sequences for overexpression or knockdown of circIFNGR2 were co-transfected with pSPAX2 and pMD2.G into 293T cells by Lipo8000 (Beyotime, Beijing, China). After collection and filtration, the supernatants were used for infecting THP-1 cells with 5 μg/mL polybrene (Beyotime, Beijing, China). Then, infected THP-1 cells were re-seeded in fresh medium and added with puromycin for 7 days. For miRNA and plasmids transfection, miR-939 mimics, miR-939 inhibitor, plvx vectors containing sequences of eIF4A3, si-eIF4A3 and controls were transfected by Lipo8000 (Beyotime, Beijing, China). qRT-PCR was used to evaluate the efficiency of infection and transfection.

RNase R treatment

Five micrograms of total RNA from THP-1 cells were treated with (RNase R+) or without (RNase R-) RNase R (3 U/mg, Epicenter, WI, USA) and incubated for 30 min at 37°C. Then, qRT-PCR analysis was used to detected the expression of circIFNGR2 and its host gene *IFNGR2* as described above.

Cell proliferation assay

BeyoClick EdU-555 kit (Beyotime, Beijing, China) was used to evaluate cell proliferation. Briefly, stably-expressed THP-1 cells were incubated with 5-ethynyl-2′-deoxyuridine (EdU) for 4 h and fixed with 4% paraformaldehyde. Then, each group of cells were re-suspended and incubated with Click reaction buffer. The

signals of EdU were detected by CytoFLEX flow cytometer (Beckman Coulter, CA, USA). Data with 3 replicates were analyzed using FlowJo software (Tree Star, OR, USA).

Western blot analysis

Total proteins were extracted from cultured cells with RIPA Lysis Buffer with 1% protease and 1% phosphatase inhibitor (Beyotime, Beijing, China). Nuclear and cytoplasmic proteins were extracted by Nuclear and Cytoplasmic Protein Extraction Kit (Beyotime, Beijing, China) following manufacturer's protocls. The concentration of extracted proteins was quantified by enhanced BCA kit (Beyotime, Beijing, China). Then, the protein samples were isolated by 4–15% SDS-PAGE pre-cast gels (Beyotime, Beijing, China) and transferred to PVDF membranes (Millipore, MA, USA). After blocked by QuickBlock Blocking Buffer for Western Blot (Beyotime, Beijing, China), the membranes were incubated with primary antibodies of iNOS (Abcam, MA, USA), TNFα (proteintech, IL, USA), IL1β (Bioss, Beijing, China), IL6 (Abcam, MA, USA), CD86 (Bioss, Beijing, China), p65 (Beyotime, Beijing, China), p-p65 (Beyotime, Beijing, China), Iκκα/β(Beyotime, Beijing, China), Akt (Abmart, Shanghai, China), *p*-Akt (Abmart, Shanghai, China), mTOR (Abmart, Shanghai, China), *p*-mTOR (Abmart, Shanghai, China), eIF4A3 (Bioss, Beijing, China), Histone H3 (Bioss, Beijing, China) and β-Tubulin (Abmart, Shanghai, China) for 12 h at 4°C. Then, the membranes were incubated with HRP-conjugated secondary antibodies (proteintech, IL, USA) and detected with BeyoECL kit (Beyotime, Beijing, China).

Flow cytometry

To determine the M1/M2 polarization, THP-1 derived macrophages were stained with iNOS/TNFα and CD163/CD206 under M1 or M2 polarization respectively. M1 macrophages were collected, washed by 1× phosphate buffer saline (PBS, Solarbio, Beijing, China) added with 3% FBS, fixed with 1% paraformaldehyde, permeabilized by Triton X-100 and stained with APC-*anti*-iNOS and PE-*anti*-TNFα. M2 macrophages were collected and washed with 1× PBS added with 3% FBS and stained with APC-*anti*-CD163 (BioLegend, CA, USA) and PE-*anti*-CD206 (BioLegend, CA, USA) were added into cells for staining. The gating for M1/M2 macrophages were presented in Figure S6. Flow cytometric data were collected on CytoFLEX flow cytometer (Beckman Coulter, CA, USA) and analyzed by FlowJo software (Tree Star, OR, USA).

Enzyme-linked immunosorbent assay (ELISA)

The secretion levels of human TNFα, IL6, IL1β and IL23 in the supernatants of cultured THP-1 derived macrophages were detected by ELISA kits (MEIMIAN, Jiangsu, China) according to the manufacturer's protocols. Optical density at the wavelength of 450 nm were measured by Infinite 200 PRO microplate reader (TECAN, Switzerland).

Dual-luciferase reporter assay

The sequences of wild-type circIFNGR2 (WT) and mutant miR-939-binding sites (Mut) were synthesized and cloned to pEZX-MT06 luciferase reporter vectors (GeneCopoeia, Guangzhou, China). Then the plasmids and miR-939 mimics and its negative controls were co-transfected into 293T cells using Lipo8000 (Beyotime, Beijing, China) respectively. The luciferase activities were measured after 48 h of transfection using the Luc-pair Duo-Luciferase HS assay kit (GeneCopoeia, Guangzhou, China).

RNA antisense purification (RAP)

To determine the binding relationships of circIFNGR2/miR-939 and miR-939/iNOS or miR-939/TNFα, RAP kits (BersinBio, Guangzhou, China) along with biotin-conjugated probes targeted circIFNGR2 and miR-939 (RiboBio, Guangzhou, China) and corresponding negative controls were used to pulled down target sequences following the manufacturer's instructions. The RNA from immunoprecipitates were extracted and the expression levels of circIFNGR2, miR-939, iNOS and TNFα were then detected by qRT-PCR. To verify the binding between eIF4A3 and flanking regions of circIFNGR2, biotin-labeled probes for upstream and downstream flanking sequences were used for hybridization in crosslinked cells as in accordance with the manufacturer's protocols. After elution, the proteins in immunoprecipitates were purified and used for detecting the expression levels of eIF4A3 by Western blot analysis as described above.

RNA immunoprecipitation (RIP)

For further confirmation of binding relationship of eIF4A3 and flanking sequences of circIFNGR2, we performed RIP assays using RIP kits (BersinBio, Guangzhou, China) following the instruction manuals. Briefly, THP-1 derived macrophages were crosslinked, removal of DNA and immunoprecipitated by anti-eIF4A3 antibody and IgG. Eventually, qRT-PCR was used to detect the expressions of potential binding sequences in flanking regions of circIFNGR2, in which lncH19 was used as positive control.

QUANTIFICATION AND STATISTICAL ANALYSIS

Each experiment was conducted in triplicate. The quantitative data with normal distribution are presented as the mean ± SD, while the data with non-gaussian distribution are shown as median and quartiles. Student's *t* test, Welch's *t*-test or Mann-Whitney U test was used for comparison of two groups depending on distribution and homoscedasticity of data. two-way ANOVA was used for multi-factorial comparisons in Arthritis Score. The correlation analysis was confirmed by Pearson's correlation. All graphs and data were generated, calculated and analyzed using GraphPad Prism 8 (GraphPad Software, CA, USA). A $p < 0.05$ was considered as statistically significant.